https://dx.doi.org/10.4314/ijs.v25i3.17

SYNTHESIS, CHARACTERISATION AND ANTIBACTERIAL STUDY OF COPPER(II) COMPLEXES OF NEW BENZYLACETONE-BENZOYLHYDRAZONE AND ITS *PARA*-NITRO AND *PARA*-HYDROXY SUBSTITUTED ANALOGUES

Ajayeoba, T. A.[1,*]., Famojuro, A.T.[1], Akinkunmi, E. O.[3], Olasehinde, O.[3], Ayeni, A. O.[1], Akinyele, O. F.[1] and Woods, J.A.O.

[1]Department of Chemistry, Obafemi Awolowo University, Ile-Ife, Nigeria.
[2]Department of Chemistry, University of Ibadan, Ibadan, Nigeria.
[3]Department of Pharmaceutical Microbiology, Obafemi Awolowo University, Ile-Ife, Nigeria.
[*]Corresponding Author's Email: tajayeoba@oauife.edu.ng
(Received: 2nd October, 2023; Accepted: 7th December, 2023)

ABSTRACT

Three new ligands *viz*, benzylacetone-benzoylhydrazone [babh (L^1)], *para*-hydroxy-benzylacetone-benzoylhydrazone [*p*-OH-babh (L^2)] and *para*-nitrobenzylacetone-benzoylhydrazone [*p*-NO_2-babh (L^3)], were synthesised by condensation of hydrazides with benzylacetone. The ligands were each reacted with copper(II) salts (chloride, nitrate, acetate and sulphate) to form complexes with the general formulae ML_2X_2 (X = Cl^-, NO_3^-, AcO^- and SO_4). The compounds were characterised using ^{1}H NMR, Infrared and UV-Visible spectroscopy, as well as CHN elemental analyser and magnetic susceptibility measurements. Antibacterial activity of the ligands and synthesised complexes were investigated using the agar diffusion method against two Gram-positive (*Staphylococcus aureus* NCTC 6571 and *Bacillus cereus* ATCC 11778) and three Gram-negative (*Escherichia coli* ATCC 25922, *Pseudomonas aeruginosa* ATCC 10145, Klebsiella *pneumonia* ATCC 13048) bacterial strains. However, the observed antimicrobial strength of the synthesized compounds was rather low.

Keywords: Benzylacetone-benzoylhydrazone, *para*-Hydroxy-benzylacetone-benzoylhydrazone, *para*-Nitro-benzylacetone-benzoylhydrazone, Antimicrobial activity, Copper(II) complexes.

INTRODUCTION

Hydrazones and their metal complexes have remained an interesting area of studies for the Inorganic and bioinorganic chemist in the last decades, due to their biological activity and industrial applications (Olurotimi *et al*., 2017; Emami *et al*., 2021; Argibay *et al*., 2022). Hydrazones are formed by condensation reactions (Figure 1) between hydrazine derivatives often called hydrazides, and carbonyl compounds (aldehyde or ketone) (El-Gammar, 2015; Ajayeoba *et al*., 2021; Argibay *et al*., 2022). These hydrazones have proven to be versatile ligands in the coordination chemistry of transition metals. Their unique structural characteristics, coupled with the ability to modulate their electronic and steric properties through functional group substitution, make hydrazine particularly intriguing candidates for metal complexation (Saeed *et al*., 2016; Meira, *et al*., 2018). In this paper, the coordination ability of the novel ligands; benzylacetone-benzoylhydrazone and its *para*-hydroxyl and *para*-nitro substituted analogues with copper(II) metal salts bearing various counter anions were explored with a view to understanding their chemistry, since it is known from literature that copper(II) complexes do exhibit distinctive structural features and electronic properties, which are influenced by the nature of the substituents on the hydrazone ligands (Kendel *et al*., 2020; Wu *et al.,* 2023). Their antibacterial activity was also investigated since hydrazones and their metal complexes are known to exhibit antimicrobial activities. In conclusion, this study endeavour to contribute to the growing body of knowledge on copper(II) complexes of hydrazones.

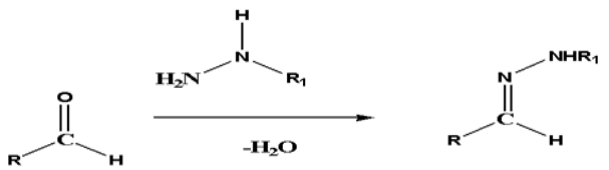

Figure 1: Formation of Hydrazones (R = Alkyl, Phenyl, Heterocyclic ring, R_1= H, Phenyl, Heterocyclic ring).

EXPERIMENTAL

Materials

Analar grade reagents and solvents were obtained from Sigma-Aldrich and British Drug Houses (BDH) Chemicals Limited. These reagents were

employed without any further purification. The melting point or decomposition temperatures of the synthesised compounds were determined utilising a Gallenkamp (variable heater) Melting Point apparatus and a Sherwood melting point apparatus. Elemental Analysis (Microanalysis) was conducted using Elemental Vario ELIII elemental analyser from Hanau, Germany. Infrared spectra for all the complexes and ligands were recorded using a Perkin Elmer FT-IR Spectrophotometer, covering the range of 4000 – 400 cm^{-1}. UV-visible electronic spectra of the ligands were measured in methanol, while the visible region for the complexes was determined through solid diffuse reflectance using quarts cuvettes on a Shimadzu UV-Vis 1800 Spectrophotometer. ^{1}H NMR spectra were obtained on a Bruker DMX advance spectrometer (300 Mhz) with internal standard. The magnetic susceptibility of the metal complexes was determined using a Sherwood Scientific Magnetic Susceptibility Balance, MSB Mark1.

Ligand Preparation

The process of preparing the hydrazones involved two distinct steps. The first step was the preparation of the precursor, namely benzoylhydrazide and their para-hydroxyl- and para-nitro- substituted derivatives. This was achieved by reacting appropriate 4- substituted alkyl esters with a solution of hydrazine hydrate under reflux conditions. In the second step, this benzoylhydrazide and its substituted derivatives were subjected to a condensation reaction with benzylacetone, to give the respective hydrazones derivatives (Ajayeoba *et al*., 2021; Adekunle *et al*., 2013)

Syntheses of Hydrazides

Benzoylhydrazide

Equimolar amount of hydrazine hydrate 19.40 mL (400 mmol) and ethyl benzoate 63 mL (400 mmol) were mixed with 150 mL ethanol in a 500 mL round bottom flask placed on a water bath. The mixture was refluxed for 12 h, resulting in a yellowish solution, which was then concentrated using a rotary evaporator to yield a white crystalline precipitate. This precipitate was filtered under suction and washed with 40% ethanol, followed by drying in a desiccator over $CaCl_2$.

p-*Nitrobenzoylhydrazide*

Equimolar amount of methyl-4-nitrobenzoate 10 g (55.20 mmol) and 2.67 mL (55.20 mmol) of hydrazine hydrate in 50 mL ethanol solvent was refluxed for 6 h. The solution was concentrated by reducing solvent volume to half of its initial amount and left overnight. A brownish yellow precipitate formed, which was then filtered under suction, washed with distilled water and 40% ethanol, and dried over $CaCl_2$ in a desiccator.

p-*Hydroxybenzoylhydrazide*

Methyl-4-hydroxylbenzoate 20 g (131.4 mmol) of was dissolved in 100 mL methanol, heated for 5 min., and then combined with 12.76 mL (262.8 mmol) of hydrazine hydrate (100% excess) mixed with 20 mL of methanol. The mixture was refluxed for 6 h and allowed to evaporate without heating. After 24 h of evaporation, a white powdery precipitate formed. This precipitate was filtered under suction, washed with 40% methanol and dried over $CaCl_2$ in a desiccator.

Equation for the reaction:

$X\text{-}RCOOR' + N_2H_4.H_2O \rightarrow X\text{-}RCONHNH_2 + R'OH + H_2O$ (X = H, OH, NO_2)

Syntheses of Hydrazones

Benzylacetone-benzoylhydrazone (babh) (L^1)

Equimolar amount of benzoylhydrazide (10.18 g, 74.76 mmol) and benzylacetone 11.20 mL (74.76 mmol) were refluxed for 6 h. The mixture was poured into a 250 mL beaker, allowing the solvent to slowly evaporate. After 24 h, a white needle-like crystalline precipitate formed. It was filtered, washed with 40% ethanol, air-dried for 20 min. and then placed in a desiccator over $CaCl_2$.

*Benzylacetone-***p***-hydroxybenzoylhydrazone (***p***-OH-babh) (L^2)*

A mixture of 10 g (65.70 mmol) of *p*-hydroxybenzoylhydrazide was dissolved in a 70/10 mL methanol/acetone mixture with 1 mL of acetic acid added as a catalyst. This mixture was reacted with benzylacetone (9.85 mL, 65.70 mmol) in 20 mL methanol and refluxed for 6 h. The solvent was reduced to half its initial volume, and after cooling for 3 h, a white crystalline precipitate formed. This precipitate was washed with 40% methanol under suction and then dried in a desiccator over $CaCl_2$.

p-*Nitrobenzylacetone-benzoylhydrazone* (**p**-NO_2-*babh*) (L^3)

Equimolar amounts of *p*-nitrobenzoylhydrazide (10 g, 55.2 mmol) and benzylacetone (8.27 mL, 55.2 mmol) were mixed in 150 mL ethanol solvent, with 3 mL of acetic acid added as a catalyst. The reaction was refluxed for 6 h and then the reaction mixture was concentrated by reducing the solvent volume to half its initial amount. After 24 h, a yellow precipitate formed which was filtered under suction, washed with 40% ethanol, and dried over $CaCl_2$ in a desiccator.

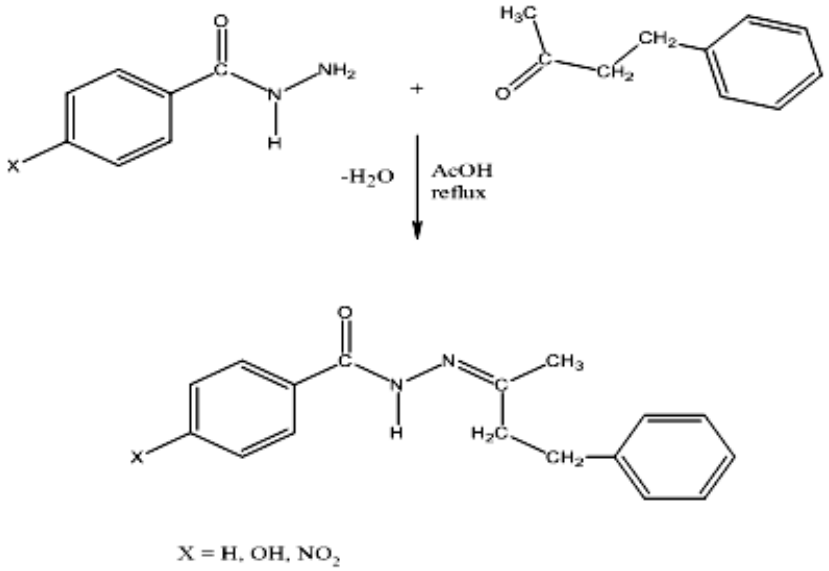

Scheme 1: Synthetic route for the ligands.

Syntheses of Metal Complexes

Copper(II) benzylacetone-benzoylhydrazone

An amount (2.00 g, 7.51 mmol) of babh (L^1) ligand dissolved in 20 mL ethanol, and (0.75 g, 3.76 mmol) of copper(II) acetate monohydrate dissolved in 20 mL of distilled water was added to the stirring mixture dropwise in a beaker. The mixture was stirred for 4 h to form a green precipitate, which was filtered, washed with 40% ethanol and dried over $CaCl_2$ in the desiccator.

Copper(II) **p**-*hydroxybenzylacetone-benzoylhydrazone*

An amount (0.50 g, 1.76 mmol) of **(L^2)** was dissolved in 30 mL of 2:1 methanol/acetone mixture, which was stirred to dissolution. Thereafter, 0.21 g (0.88 mmol) of Cu(II) nitrate tetrahydrate in 10 mL of methanol was added to the stirring solution. The mixture was stirred for 1 h to give a green precipitate. It was filtered, washed with distilled water, and then with acetone/methanol mixture. The precipitate was dried in the desiccator over $CaCl_2$.

All metal(II) complexes of *p*-hydroxyl-benzylacetone-benzoylhydrazone and *p*-nitro-benzylacetone-benzoylhydrazone were prepared in a similar manner.

$$MY_2.nH_2O + RCONHN=CR_1R_2 \rightarrow [M(RCONHN=CR_1R_2)_2(Y)_2].nH_2O$$

Scheme 2: Synthesis of metal(II) complexes.

Where, M = Cu(II) ; Y = Cl, NO_3, OAc and SO_4

Qualitative Assessment of Antimicrobial Activity (Agar Diffusion Technique)

The susceptibility of the organisms to the newly synthesised hydrazones was determined using bioassay method as described by Akinkunmi *et al*., 2014. The following bacterial strains were used, *viz, Staphylococcus aureus* NCTC 6571, *Bacillus cereus* ATCC 11778, *Escherichia coli* ATCC 25922, *Pseudomonas aeruginosa* ATCC 10145 and Klebsiella *pneumonia* ATCC 13048. Solutions of known concentrations (10 mg/mL) of the compounds were prepared by dissolution in 20 % DMSO (also used as negative control), while streptomycin (0.125 mg/mL) was used as positive control. Bacteria were kept on nutrient agar slants at 4 °C. A total of 20 mL of molten Mueller Hinton agar (Oxoid) was poured into individual sterile petri-dishes and left to solidify. The surface of the agar was then swabbed with a 24-h broth culture of the bacteria strain, which had been diluted to a concentration of 10^6 colony forming units per

milliliter (cfu/mL) using a sterile cotton swab.

Using a cork-borer that had been flamed and cooled, wells were created in the agar plates, and the removed plugs were discarded in a asceptic manner. Subsequently, the plates were incubated for 1 h. After this initial incubation, 0.2 mL of a compound with a concentration of 10 mg/mL was added to each well using a sterile calibrated dropper. The plates were then left on the bench for an additional hour to allow the compounds to diffuse into the agar.

Following this diffusion period, the plates were then incubated for 24 h at 37 °C. The diameters of the zones of inhibition were measured using a transparent ruler in mm. The summarised results can be found in Table 7.

Crystal structure determination

Needle-shaped, single, white crystals of the hydrazone ligand obtained in ethanol medium were selected and subjected to X-ray crystallographic analysis. "Bruker KAPPA APEX II single crystal X-ray diffractometer equipped with a 4-circle kappa goniometer and a CCD detector at 296(2) K was used in the collection of crystal data. The instrument consisted of a molybdenum fine focus sealed X-ray tube as an X-ray source and an Oxford cryostream 700 system for sample temperature control (Sheldrick, 2015). The structure was solved using SHELXT-2014 (Sheldrick, 2015) and refined by least square procedures using SHELXL-2016 with SHELXLE (Hubschle *et al.*, 2011) as a graphical interface. Data were recorded for absorption effects using the numerical method implemented in SADABS. All non-hydrogen atoms were refined anisotropically while all hydrogen atoms were refined isotropically. Details on the crystallographic data can be found as supplementary materials in the Cambridge Crystallographic Data Centre (CCDC: 2118166). The data can be requested at no cost via www.ccdc.cam.ac.uk/data_request/cif

RESULTS AND DISCUSSION

The hydrazone ligands and copper(II) complexes were synthesized using previously described method in literature (Gup and Kirkan, 2005; Rodriquez–Arguelles, 2009; Cao *et al.*, 2018a), and were characterised to determine their stoichiometry and geometry, as presented in Table 4. The compounds babh (L^1) and *p*-OH-babh (L^2) are white, while *p*-NO_2-babh (L^3) has a yellowish colour. The copper(II) complexes showed colours ranging from green to blue to brown. The melting points of the hydrazone ligands ranged from 132 – 220 °C, while those of the copper(II) complexes was between 140–300 °C, with three complexes surpassing 300 °C. The complexes generally exhibited high thermal stability (Meira *et al.*, 2018). The trend in the melting points of the complexes based on the counter anions present followed the order: Sulphate ≅ Chloride > Nitrate > Acetate. Metal analysis results demonstrated a good agreement between expected and observed values, revealing a 1:3, 1:2 and 1:1 (M: L) ratio for the complexes. Results of the microanalysis were generally in agreement with the stoichiometry. This result conformed to the observation that the anions were present in the complexes and that some of the compounds were hydrated. Some of the few discrepancies may be attributed to solvent presence.

X-ray data analysis for (L^1)

The ORTEP diagram of the ligand is presented in Figure 2a, with the crystallographic data summarized in Table 1. The summary of bond interactions of the hydrazone functional group is presented in Table 2. The compound crystallizes as a hydrate (Figure 2a) which have been previously reported for similar *N*-aroyl hydrazones derivatives [Hubschle *et al.*, 2011; Mazur *et al.*, 2014). Table 1 shows that the compound crystallizes as a triclinic in the centrosymmetric space group P_{-1}, with one hydrazone in the asymmetric part of the crystal unit (Figure 2a), coupled with intermolecular hydrogen bonding linking crystal lattices. The crystal structure shows the hydrazide function adopt the cis conformation, which is consistent with other N-aroylhydrazones derivatives reported in the literature (Mazur *et al.*, 2014). In the synthesized ligand babh, the mean value for the azomethine (C=N) double bond distance is determined to be 1.32(6) Å, which is for doubly bond which suggest elongation of the N1-C9 bond due to the electron donating properties of the methyl groups substituents on the azomethine

carbon. This phenomenon has been previously predicted for hydrazone with electron-donating substituents (Mador *et al*., 2019). The mean bond distance between atoms C11 and N2 is 1.37(6) Å indicates a singly bond, which is similar for values obtained for structurally related compounds (Simone *et al*., 2010; Ajayeoba *et al*., 2021). The stability of the compound was enhanced by the intermolecular hydrogen bonding and the pi-pi stacking of the phenyl rings. The geometrical parameters of the ligand babh are similar with other structurally related hydrazones reported in the literature (Marcos *et al*., 2010).

Table 1: X -ray diffraction data collection and refinement parameters for babh

Identification code	babh
Empirical formula	$C_{17}H_{18}N_2O$
Formula weight	266.34
Temperature/K	296(2)
Crystal system	triclinic
Space group	P_{-1}
a/Å	14.103(2)
b/Å	15.298(2)
c/Å	16.325(2)
α/°	64.063(5)
β/°	77.115(6)
γ/°	76.550(6)
Volume/Å^3	3050.7(7)
Z	39
ϱ_{calc}g/cm^3	1.162
μ/mm^{-1}	0.073
F(000)	1138.0
Crystal size/mm^3	0.280 × 0.170 × 0.080
Radiation	MoKα (λ = 0.71073)
2Θ range for data collection/°	3.898 to 179.172
Index ranges	-19 ≤ h ≤ 19, 19 ≤ k ≤ 19, 42 ≤ l ≤ 42
Reflections collected	76863
Independent reflections	16992 [R_{int} = 0.0395, R_{sigma} = 0.0403]
Data/restraints/parameters	16992/0/721
Goodness-of-fit on F^2	11.139
Final R indexes [I>=2σ (I)]	R_1 = 0.7123, wR_2 = 0.9226
Final R indexes [all data]	R_1 = 0.7371, wR_2 = 0.9333
Largest diff. peak/hole / e Å^{-3}	2.77/-2.26

Table 2: Selected bond lengths (d) and bond angles (θ) for the compound babh after Refinement

d	**(Å)**	θ	**(deg)**
O1–C11	1.323(19)	O1–C11–N2	113(2)
N2–C11	1.16(4)	N2–C11–C12	120.2(16)
N2–N1	1.55(4)	C9–N1–N2	114(4)
NI–C9	1.47(6)	N1–C9–C8	104(2)
C9–C8	1.62(5)	O1 – C11 – C12	126(2)
C9–C10	1.39(4)	N1 -C9 – C10	121.9(19)

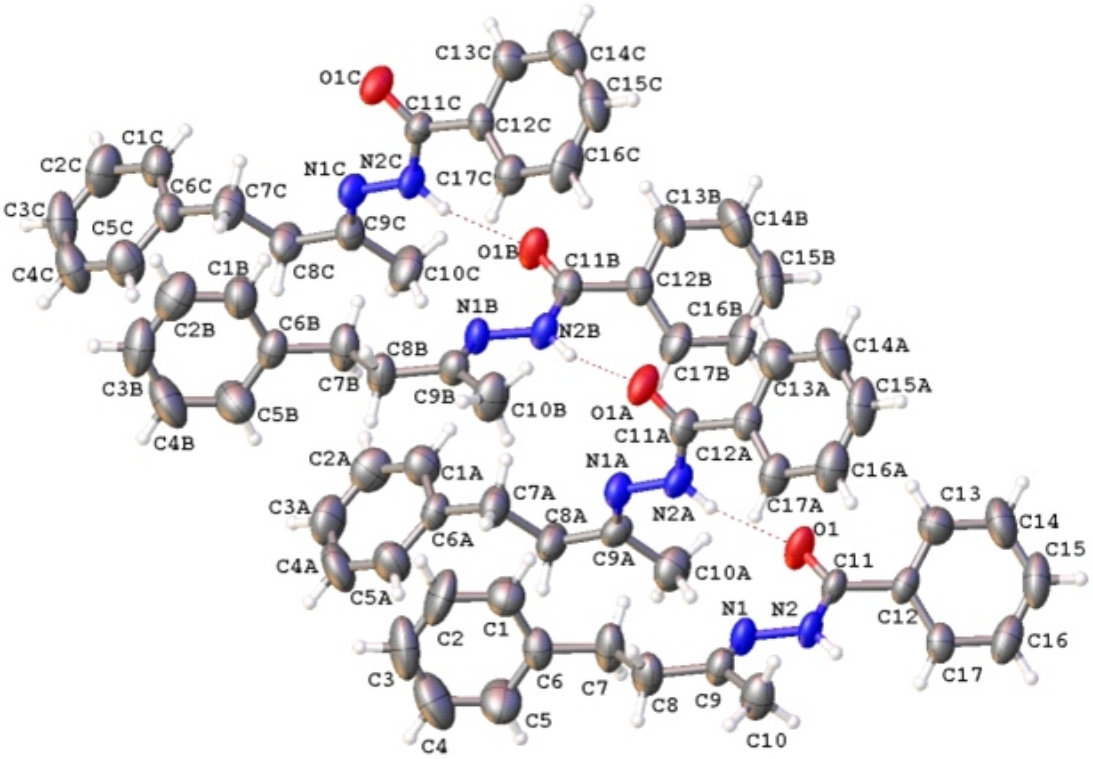

Figure 2a: ORTEP numbering of the crystal packing showing the intermolecular hydrogen bonding

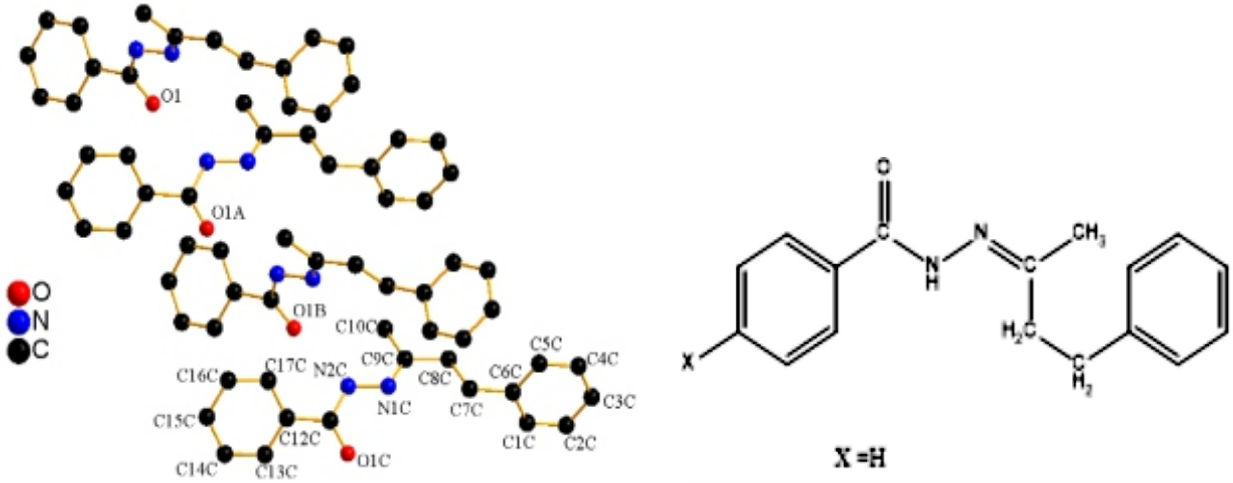

Figure 2b: Structure of benzylacetone-benzoylhydrazone (L^1).

^{1}H-NMR

The ^{1}H-NMR spectra gave insight into the structure of benzylacetone-benzoylhydrazone (L^1), its *para*-hydroxyl (L^2) and *para*-nitro (L^3) substituted analogues. The data are presented in Table 3 and spectrum of L^1 shown in Figure 3. These ligands typically exhibited five sets of peaks. The first set appearing as a singlet at 10.40 ppm (1H, s) in L^1, 9.90 ppm (1H, s) in L^2 and 11.20 ppm (1H, s) in L^3 was assigned to the hydrazono (N-H) proton and is a diagnostic feature of hydrazones as reported in previous studies (Chitrapriya *et al*., 2008; Gup *et al*., 2015; Saeed *et al*., 2016). The upfield signal in *p*-OH-babh (L^2) was the result of electron donating effect of the hydroxy group shielded the proton, while in *p*-NO_2-babh (L^3), the downfield shift was due to the electron withdrawing effect of the nitro group, making the hydrazono proton more deshielded (Al-Sha'alan, 2011). In addition to the (N-H)

signals, L^2 showed a signal at 10.10 ppm (1H, s) corresponding to O-H. These signals appeared at higher δ values due to their attachment to electronegative atoms, which are oxygen and nitrogen, suggesting the possibility of extensive hydrogen bonding (Beves *et al*., 2009; Ajayeoba, 2019). The second set of signals appeared as a multiplet in the range of 7.10 -7.80 ppm (10 H, multiplet) in (L^1); 6.70 – 7.70 ppm (9 H, multiplet) in (L^2) and 7.60 -8.80 ppm (9 H, multiplet) in (L^3) corresponding to the aromatic protons (Saeed *et al*., 2016). The third group consisted of two adjacent methylene groups, each appearing as triplet in the range 2.50–2.60 ppm for babh (L^1), 2.60 – 2.80 ppm for *p*-OH-babh (L^2), and 3.00 - 3.10 ppm in *p*-NO_2-babh (L^3). The methyl group was observed as a singlet at 1.90 ppm (1 H, s) in L^1, at 1.90 ppm (1 H, s) in L^2 and underwent a significant shift to 3.80 ppm (1H, s) in L^3.

It was apparent from the ^{1}H-NMR spectra of the ligands that the keto form was the predominant species in solution, while the enol form was limited, which was also evident in the composition of the metal(II) complexes.

Table 3: The ^{1}H NMR data of the ligands.

Compounds	δ (ppm)	Signal	No of protons	Attribution
L^1	1.90	Singlet	(3, H)	CH_3
	2.60	Triplet	(2, H)	CH_2
	2.80	Triplet	(2, H)	CH_2
	7.10 – 7.80	Multiplet	(10, H)	Aromatic protons
	10.40	Singlet	(1, H)	N-H
L^2	1.90	Singlet	(3, H)	CH_3
	2.50	Triplet	(2, H)	CH_2
	2.80	Triplet	(2, H)	CH_2
	6.70 – 7.70	Multiplet	(9, H)	Aromatic protons
	9.90	Singlet	(1, H)	N-H
	10.10	Singlet	(1, H)	O-H
L^3	3.80	Singlet	(3, H)	CH_3
	3.00	Triplet	(2, H)	CH_2
	3.10	Triplet	(2, H)	CH_2
	7.60 – 8.80	Multiplet	(9, H)	Aromatic protons
	11.20	Singlet	(1, H)	N-H

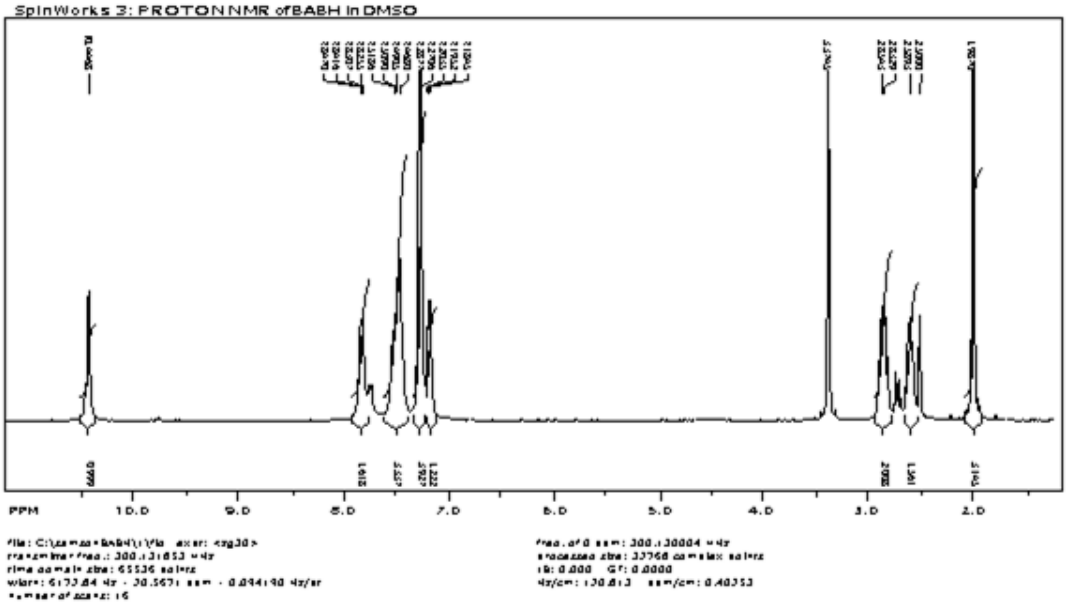

Figure 3: ^{1}H NMR of benzylacetone-benzoylhydrazone (L^{1}).

Table 4: Physical properties and analytical data for babh compounds.

Compound	Formula (M. wt)	Mp/dec. temp.	Yield (%)	Carbon (%)	Hydrogen (%)	Nitrogen (%)	Metal (%)	μ_{eff}(BM
Babh (L^1) (White)	$C_{17}H_{18}N_2O$ (266.34)	130-132	92	76.67 (76.66)	7.34 (6.81)	10.66 (10.51)	-	-
p-OH-babh (L^2) (White)	$C_{17}H_{18}N_2O_2$ (282.33)	147-149	89	72.33 (72.31)	8.01 (6.43)	9.41 (9.92)	-	-
p-NO_2–babh (L^3) (Yellow)	$C_{17}H_{17}N_3O_3$ (311.34)	218-220	96	65.24 (65.58)	6.81 (5.50)	13.92 (13.50)	-	-
$Cu_2(L^1)_2Cl_2$ (Brown)	$C_{34}H_{36}N_4O_2Cl_2Cu_2$ (730.76)	>300	41	55.96 (55.88)	5.98 (4.96)	9.27 (9.66)	8.56 (8.69)	2.90
$Cu(L^1)(NO_3)_2.5H_2O$ (Blue)	$C_{17}H_{28}N_4O_{12}Cu$ (543.96)	139-140	54	36.68 (37.54)	3.78 (5.14)	10.66 (10.51)	10.93 (11.68)	2.09
$Cu(L^1)_3(OAc)_2$ (Green)	$C_{55}H_{60}N_6O_7Cu$ (980.64)	188-190	69	68.42 (67.34)	9.35 (6.17)	9.95 (8.57)	6.31 (6.48)	2.43
$Cu(L^1)_2SO_4.H_2O$ (Brown)	$C_{34}H_{38}N_4O_7SCu$ (710.23)	>300	31	57.26 (57.49)	6.51 (5.35)	11.25 (11.89)	8.72 (8.94)	2.24
$Cu(L^2)_2Cl_2$ (Green)	$C_{34}H_{36}N_4O_4Cl_2Cu$ (700.29)	191-193	77	58.18 (58.31)	6.11 (5.18)	7.88 (8.00)	9.43 (9.07)	1.92
$Cu(L^2)_2(NO_3)_2$ (Green)	$C_{34}H_{36}N_6O_{10}Cu$ (752.22)	205-207	82	54.80 (54.29)	5.60 (4.79)	11.20 (11.17)	8.39 (8.44)	1.88
$Cu(L^2)_2(OAc)_2$ (Brown)	$C_{38}H_{42}N_4O_8Cu$ (746.30)	197-199	63	65.02 61.65	6.65 (5.67)	8.98 (7.50)	8.46 (8.51)	1.98
$Cu(L^2)SO_4.3H_2O$ (Green)	$C_{17}H_{24}O_9N_2SCu$ (495)	234-236	38	40.87 (41.17)	5.47 (4.88)	9.60 (5.65)	12.69 (12.81)	2.18
$Cu(L^3)Cl_2.2H_2O$ (Green)	$C_{17}H_{21}N_3O_5Cl_2Cu$ (481.91)	226-228	31	33.88 (42.37)	3.51 (4.39)	11.23 (11.72)	11.50 (13.18)	2.35
$Cu(L^3)(NO_3)$ (Light green)	$C_{17}H_{17}N_4O_6Cu$ (436.88)	< 300	62	48.05 (46.74)	4.51 (3.92)	16.53 (16.88)	12.86 (14.54)	1.71
$Cu((L^3)_3(OAc)_2$ (Green)	$C_{55}H_{57}N_9O_{13}Cu$ (1115.63)	210-212	73	60.16 (59.21)	7.12 (5.15)	13.34 (13.30)	6.02 (5.70)	2.27
$Cu(L^3)SO_4.2C_2H_5OH$ (Green)	$C_{21}H_{29}N_3O_9SCu$ (563.02)	212-214	79	45.53 (44.80)	4.67 (5.19)	13.40 (13.46)	10.70 (11.29)	1.89

Infrared Spectra

The infrared spectra of the synthesized hydrazone ligands and copper(II) complexes are presented in Table 5. Typically, four key bands play a significance role in interpreting the infrared spectra of hydrazone compounds (Akinyele *et al.*, 2019; Al-Ne'aimi and Al-Khuder, 2013). These bands correspond to the vibrational frequencies of ν(C=O), ν(N-H), ν(C=N) and ν(N-N).

Therefore, in the case of the newly synthesized hydrazone ligands, the ν(N-H) vibrational frequencies were observed in L^1 at 3165 cm^{-1}. In L^2, this band shifted to a lower wavenumber at 3132 cm^{-1}, which is a bathochromic shift caused by the positive inductive effect (+I) of the hydroxy substituent on the system. Similar effects were observed in the spectrum of 1-(phenyl-hydrazono)-propan-2-one, where the presence of an alkyl group (electron donating substituent) on para position, led to the lowering of the ν(N-H) band by a magnitude of 3 - 5 cm^{-1} (El-Sherif, 2009). In the infrared spectrum of L^3, the ν(N-H) stretching vibration appeared at a higher wavenumber of 3225 cm^{-1}, which is a hypsochromic shift attributed to the combination of –I inductive effect and mesomeric effect of the para-nitro substituent in the ligand (El-Sherif, 2009; Christie *et al.*, 2010).

In the copper(II) complexes, the ν(N-H) band generally had a bathochromic shift to lower wave numbers which is indicative of complexation the Cu(II) ion to the ligands. The magnitude of the lowering of this band is between (10 - 100 cm^{-1}) and is highest in copper(II) complexes of *p*-OH-babh, resulting from the +I inductive effect of the substituents. The presence of counter ions also influenced the ν(N-H) band shift, with the trend in order of acetato > chloro > sulphato > nitrato complexes. However, the ν(N-H) band had a hypsochromic shift to 3326 cm^{-1} in the spectrum of Cu(*p*-NO_2-babh)Cl_2.H_2O but no shift was observed in Cu(*p*-OH-babh)SO_4.$3H_2O$. The presence of the ν(N-H) band in the spectra of copper(II) complexes indicated that the ligands coordinated primarily in keto form, except in Cu_2(babh)$_2Cl_2$ and Cu(*p*-NO_2-babh)(NO_3) where the ν(N-H) vibrational frequencies disappeared due to enolisation of the hydrazono proton and subsequent coordination as a uninegative ligand. The appearance of a new band around 1600 cm^{-1} due to new (C=N-N=C) in these two complexes supported these findings (Cao *et al.*, 2018b).

The spectra of the metal complexes also exhibited absorption bands associated to metal-ligand vibrations, with bands in the range 500 - 666 cm^{-1} and 373 - 500 cm^{-1} assigned to the ν(M-O) and ν(M-N) modes, respectively. These bands were previously not observed in the spectra of the ligands which further suggest the coordination of the ligands to the metal ions (Akinyele *et al.*, 2020).

The coordination of nitrate, acetate and sulphate anion ligands has been extensively studied in the infrared spectra of metal complexes (Chitrapriya *et al.*, 2008; Seleem, 2011). In the sulphato complexes, a broad band around 1074 - 1090 cm^{-1} indicates coordination of the SO_4^{2-} to the metal ion. Coordination in bidentate fashion is known to decrease the tetrahedral symmetry of the group and therefore split the band. In the sulphato complexes, the band at 1080 cm^{-1} was observed to split into two, indicating the coordination of the sulphate ion to the metal(II) in a bidentate fashion (Eflhymiou *et al.*, 2009). Similarly, the acetate ions are characterized by bands at 1578 cm^{-1} and 1411 cm^{-1}, assigned to asymmetric ν_{as}(COO) and the symmetric ν_{sym}(COO) stretching vibrations of the carboxylate groups respectively (Patel *et al.*, 2013; Shebl *et al.*, 2014). In the synthesised acetato complexes, the frequencies of ν_{asy}(COO) appeared in the range 1417 – 1602 cm^{-1}, while those of ν_{sym}(COO), ranged from 1274 - 1495 cm^{-1}. The difference in Δν (ν_{asy} - ν_{sym}) has been used to determine the modes of coordination of the acetate group (Shebl *et al.*, 2014). A difference of less than 200 cm^{-1} indicate a bidentate coordination, while a difference greater than 200 cm^{-1} indicate monodentate binding. In the synthesised acetato complexes, a difference of greater than 200 cm^{-1} was found, indicating a monodentate coordination for the acetate group except in Cu(babh)$_3$(OAc)$_2$, Cu((*p*-NO_2-babh)$_3$(OAc)$_2$ where it was probable that the acetate ions were present in the outside coordination sphere. In the nitrato complexes, the presence of the nitrate ion is characterised by the

two bands in the range 1445 - 1500 cm^{-1} (symmetric stretching mode, v_4) and 1350 – 1400 cm^{-1} (asymmetric stretching mode, v_1). The presence of these bands has been used to suggest that the nitrate ion is covalently bonded and present inside the coordination sphere (Shebl *et al.*, 2014). The difference between the two bands $\Delta\nu = (\nu_{asy} - \nu_{sym})$, have been used to indicate the mode of bonding. A difference of less than 200 cm^{-1} suggest monodentate binding, while a value greater than 200 cm^{-1} indicate bidentate binding (Patel *et al.*, 2013). Therefore, in the nitrato complexes, a difference of less than 200 cm^{-1} was observed and this suggested the binding of nitrate anions as a monodentate.

Table 5: Infrared vibrational frequencies for ligands and copper(II) complexes.

Compounds	ν(O-H)/H_2O	ν(N-H)	ν(C=O)	ν(C=N)	ν(N-N)	M-O	M-N	Counter ion vibrations
L^1	-	3156	1652	1537	1030	-	-	-
L^2	3295	3132w	1652m	1607	1060	-	-	-
L^3		3225m	1667s	1602m	1060w	-	-	-
$Cu_2(L^1)_2Cl_2$	-	-	-	1524	1029	608	471	-
$Cu(L^1)(NO_3)_2.5H_2O$	3400b	3122w	1644s	1554m	1025w	509w	451w	$\nu_{4\ (1491)}$, $\nu_{1\ (1315)}$, $\nu_{2(1025)}$
$Cu(L^1)_3(OAc)_2$	-	3055	1611w	1544m	1025w	571w	493w	$\nu_{1,(1590)}$, $\nu_{2\ (1333}$
$Cu(L^1)_2SO4.H_2O$		3145vw	1601m	1522s	1000m	470	396	$\nu_{3\ (1074)}$, $\nu_{4\ (608)}$
$Cu(L^2)_2Cl_2$	3296w	3054m	1677w	1558s	927w	619w	439w	-
$Cu(L^2)_2(NO_3)_2$	3296w	3122b	1601m	1554s	926m	634w	434w	$\nu_{4,\ (1508)}$,$\nu_{1,(1343)}$,$\nu_{3,(1034)}$
$Cu(L^2)_2(OAc)_2$	3296w	3085b	1609s	1531s	934m	661m	414w	$\nu_{1,\ (1515)}$ $\nu_{2,\ (1340)}$
$Cu(L^2)SO_4.3H_2O$	3222b	3132w	1647w	1555m	958m	624w	526w	$\nu_{3,\ (1088)}$, $\nu_{4,\ (610)}$
$Cu(L^3)Cl_2.2H_2O$	3448m	3326m	1616w	1561m	1009w	614w	539w	-
$Cu(L^3)(NO_3)$	-	-	1617w	1515s	1009m	673w	593m	$\nu_{4\ (1403)}$, $\nu_{1\ (1334)}$, $\nu_{3(1004)}$
$Cu((L^3)_3(OAc)_2$	-	3179w	1615m	1517s	1012w	611m	576m	$\nu_{1\ (1595)}$, $\nu_{2\ (1341)}$
$Cu(L^3)SO_4.2C_2H_5OH$		3170w	1658w	1557m	1010m	664w	577w	$\nu_{3\ (1156)}$, $\nu_{4\ (620)}$

Electronic Spectra and Magnetic Measurements

The ultraviolet spectra of the synthesised ligands, exhibited two prominent electronic transitions (Table 6). These transitions include the intraligand $\pi \rightarrow \pi^*$ transition occurring within the aromatic system in the range 48,780 – 48,309 cm^{-1} (Agarwal *et al.*,2006; Cao *et al.*, 2018), and the bands in the range 38,460 – 37,195 cm^{-1} which resulted from the overlap of the intraligand $\pi \rightarrow \pi^*$ and $n \rightarrow \pi^*$ transitions, within the C=N-NH-CO moiety (Gup *et al.*, 2015, Mostafa, 2011). In L^1, the intraligand $\pi \rightarrow \pi^*$ transition occurred in babh at 48,780 cm^{-1} and exhibited a slight bathochromic shift to 48,309 cm^{-1} in L^2 and to 48,544 cm^{-1} in L^3. The second prominent transition arising from the overlap of the $n \rightarrow \pi^*$ and $\pi \rightarrow \pi^*$ electronic transitions in the uncoordinated hydrazone ligands occurred at 38,460 cm^{-1} and shifted to a lower wavenumber in L^2 to 37,195 cm^{-1} and to 37,313 cm^{-1} in L^3. The red shifts were attributed to the +I inductive effect of the hydroxyl substituent and –I inductive effect of the nitro substituent on the system (Gup *et al.*, 2015).

In the ultraviolet electronic spectra of the copper(II) complexes, the intraligand band $\pi \rightarrow \pi^*$ had a bathochromic shift and followed the order $Cu(L^1)_3(OAc)_2 > Cu(L^2)_2(OAc)_2 > Cu(L^2)_2Cl_2 > Cu(L^3)SO_4.2C_2H_2OH > Cu(L^1)_2SO_4.H_2O$. This shift was a result of the expansion of the d electron clouds as a result of d orbitals overlap with the orbitals of ligand atoms (Cotton *et al.*, 2003). On the other hand, all the other copper(II) complexes had a hypsochromic shift with the order being $Cu(L^3)Cl_2.2H_2O > Cu(L^3)(NO_3) > Cu(L^3)_3(OAc)_2 > Cu_2(L^1)_2Cl_2 > Cu(L^2)SO_4.3H_2O$. These shifts in the complexes were an indication of interaction between the metal(II) ions and the ligands (Omoregie and Woods, 2011; Alhadi *et al.*,

2012)

The room temperature magnetic moment for copper(II) complexes species with S = ½ usually observed for magnetically dilute copper(II) complexes is in the range 1.70 – 2.20 B. M (Chung *et al*., 1999; Omoregie and Woods, 2011; Shebl *et al*., 2014). A moment in the range 1.71 – 2.43 B. M. was observed in the copper(II) complexes which agrees with the values expected for monomeric, and magnetically dilute octahedral copper(II) complexes (Nakamoto, 1997.; Alhadi *et al*., 2012). There is however, the possibility of strong ferromagnetic interaction between the complexes that displayed higher than expected values. Furthermore, it was observed that dimeric complex $Cu_2(L^1)_2Cl_2$ had a moment of 2.90 B. M. This high value compared with the expected spin only value of 1.70 B.M for copper(II) is as a result of strong ferromagnetic coupling interaction between the two copper centres. This fact suggested that the chloro atoms are in a bridging mode between the dimeric Cu(II) complexes (Lakshmi *et al.,* 2011; Omoregie. and Woods, 2011).

Table 6: The UV-Visible electronic spectral data for the compounds.

Compounds	Intraligands transitions cm^{-1}	Ligand field transition cm^{-1}	Tentative Assignment	Proposed structure
L^1	48,780, 43,956 sh, 38,460	-	-	-
$Cu_2(L^1)_2Cl_2$	49261, 44,444	19,607 15,385 11,111	$^2B_{1g} \rightarrow {}^2B_{2g}$, $^2B_{1g} \rightarrow {}^2A_{1g}$ $^2B_{1g} \rightarrow {}^2E_g$	Square Planar
$Cu(L^1)(NO_3)_2.5H_2O$	48780, 42550, 36764sh	14,492	$^2E_g \rightarrow {}^2T_{2g}$	Octahedral
$Cu(L^1)_3(OAc)_2$	48309, 42553, 35714	16,393	$^2E_g \rightarrow {}^2T_{2g}$	Octahedral
$Cu(L^1)_2SO_4.H_2O$	44,444, 33,333	19,607	$^2E_g \rightarrow {}^2T_{2g}$	Octahedral
L^2	48309, 37195	-	-	-
$Cu(L^2)_2Cl_2$	46296, 38462	16,666 14,285 sh	$^2B_{1g} \rightarrow {}^2A_{1g}$ $^2B_{1g} \rightarrow {}^2E_g$	Octahedral
$Cu(L^2)_2(NO_3)_2$	49261, 35971	16,666	$^2E_g \rightarrow {}^2T_{2g}$	Octahedral
$Cu(L^2)_2(OAc)_2$	46948, 35714	16393	$^2E_g \rightarrow {}^2T_{2g}$	Octahedral
$Cu(L^2)SO_4.3H_2O$	48780, 37175	16,666	$^2E_g \rightarrow {}^2T_{2g}$	Octahedral
L^3	48544, 37313	-	-	-
$Cu(L^3)Cl_2.2H_2O$	49751, 39063	15,385	$^2E_g \rightarrow {}^2T_{2g}$	Octahedral
$Cu(L^3)(NO_3)$	49751, 46083sh, 37735	16,666	$^2E_g \rightarrow {}^2T_{2g}$	Octahedral
$Cu(L^3)_3(OAc)_2$	48780, 38461, 32362	15,384	$^2E_g \rightarrow {}^2T_{2g}$	Octahedral
$Cu(L^3)SO_4.2C_2H_5OH$	48076, 38461	16,666	$^2E_g \rightarrow {}^2T_{2g}$	Octahedral

Antimicrobial Activity

The results of antibacterial activity of the newly synthesised ligands and the active copper(II) complexes at a concentration of 10 mg/mL are presented in Table 7. The ligands were found to be inactive against the tested bacterial, however, in the tested copper(II) complexes, $Cu(L^1)(NO_3)_2.5H_2O$ inhibited all the tested gram-positive and gram- negative organisms except *P. aeruginosa,* while $Cu(babh)_3(OAc)_2$ inhibited the Gram – positive bacteria and Eschericia coli which is a gram-negative bacterium (Anacona and Rincones, 2015; Akinkunmi *et al*., 2014). The positive control, streptomycin however had better activity than the synthesised ligands and complexes.

Table 7: Antimicrobial activity data for the ligands and active complexes (10 mg/mL) and positive control (0.125 mg/mL).

	Zones of inhibition (mm)					
Organisms	L^1	L^2	L^3	$Cu(L^1)_3(OAc)_2$	$Cu(L^1)(NO_3)_2.5H_2O$	Strept
B. cereus (ATCC 11778)	00	00	00	30	12	32
S. aureus (NCTC 6571)	00	00	00	16	14	30
P. aeruginosa (ATCC 10145)	00	00	00	00	00	20
E. coli (ATCC 25922)	00	00	00	26	14	26
K. pneumonia (ATCC 13048)	00	00	00	20	00	26

CONCLUSION

This study reported the synthesis of a set of new hydrazone ligands, namely benzylacetone benzoylhydrazone (L^1); its *para*-hydroxyl (L^2) and *para*-nitro (L^3) analogues, and their copper(II) complexes bearing various counter ions. The copper(II) complexes had colours ranging from green, blue to brown. The complexes had high melting/decomposition temperatures indicating a high thermal stability. The presence of the proton of the N-H bond confirmed the formation of the organic ligand. The NMR studies further indicated that the ligands predominantly existed in keto form in solid state and in solution.

Infrared spectroscopy (IR) of both the ligands and the copper(II) complexes revealed that the ligands coordinated to the metal(II) ions as bidentate ligands in their keto for, however, exceptions were observed in $Cu_2(L^1)_2Cl_2$, $Cu(L^3)(NO_3)$ where the ligands coordinated in enolised form, acting as a uninegative bidentate ligand.

Based on electronic spectral data and magnetic moment measurement, the Cu(II) complexes appeared to have a probable six coordinate octahedral geometry, except $Cu_2(L^1)_2Cl_2$ and $Cu(L^3)(NO_3)$ that had a probable four coordinate square planar geometry.

The sensitivity study indicated that the synthesized ligands generally showed inactivity against all the microorganisms at a concentration of 40 mg/mL used for the screening test. and the copper(II) complexes had very low antibacterial activity against the identified organisms.

Proposed Structure

(a)

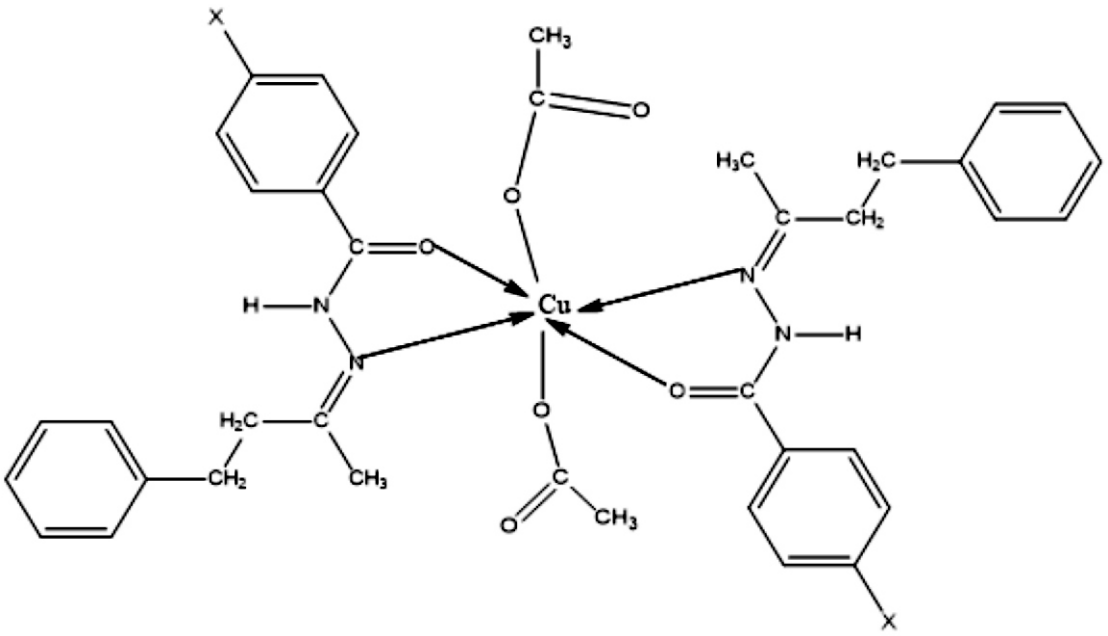

(b)

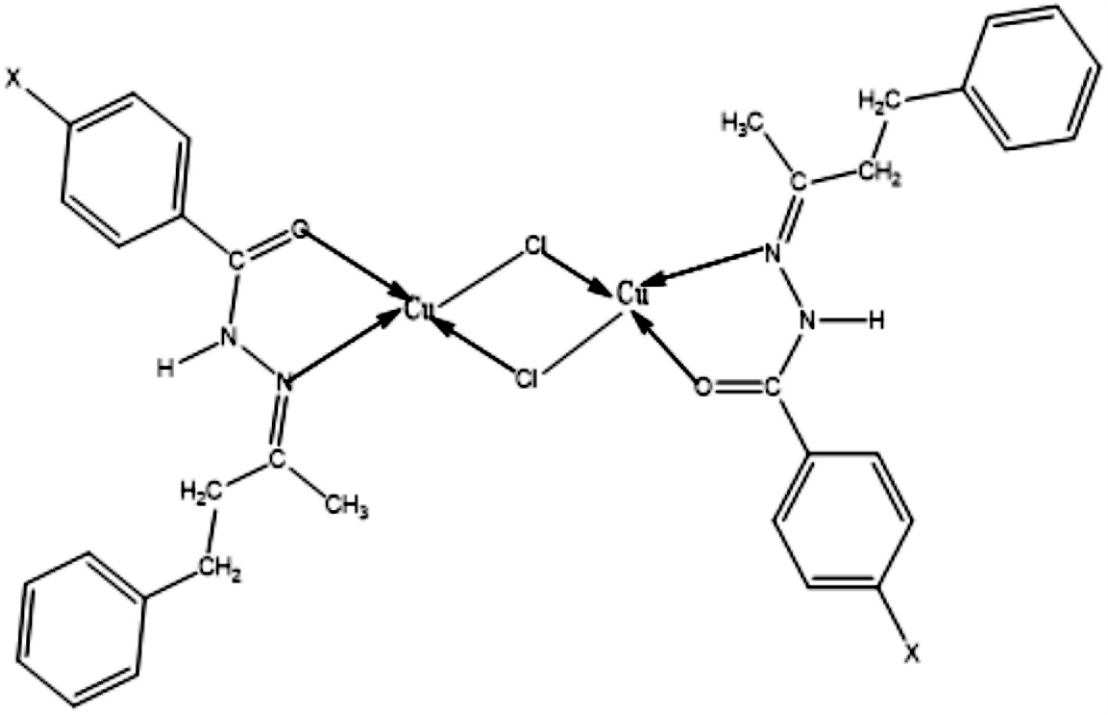

(c)

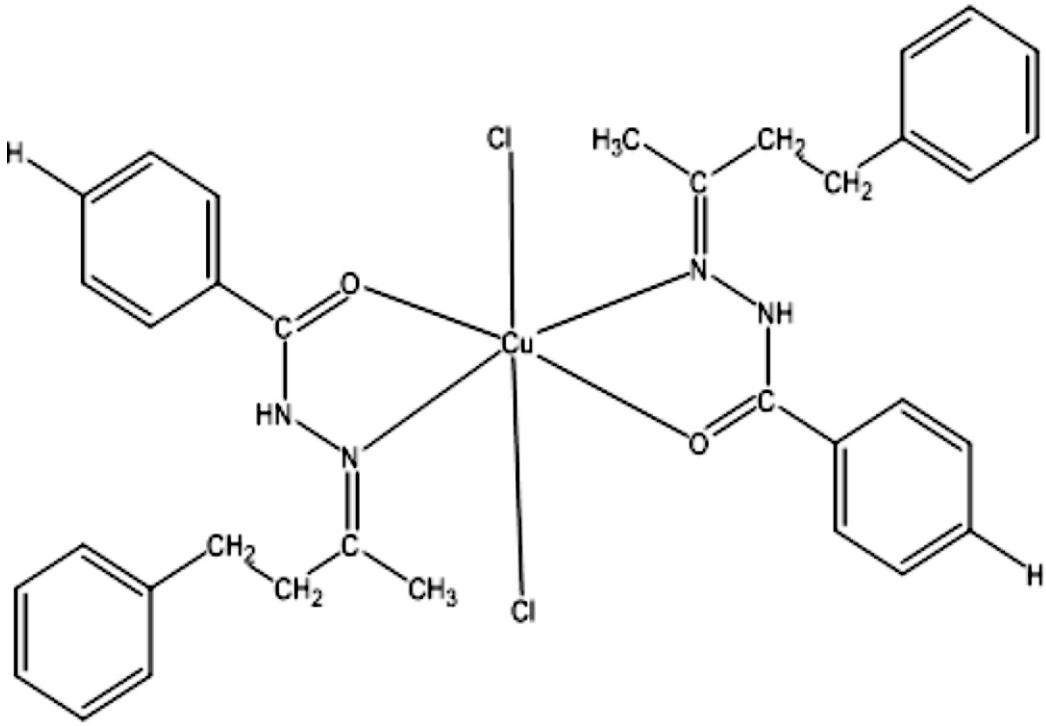

(d)

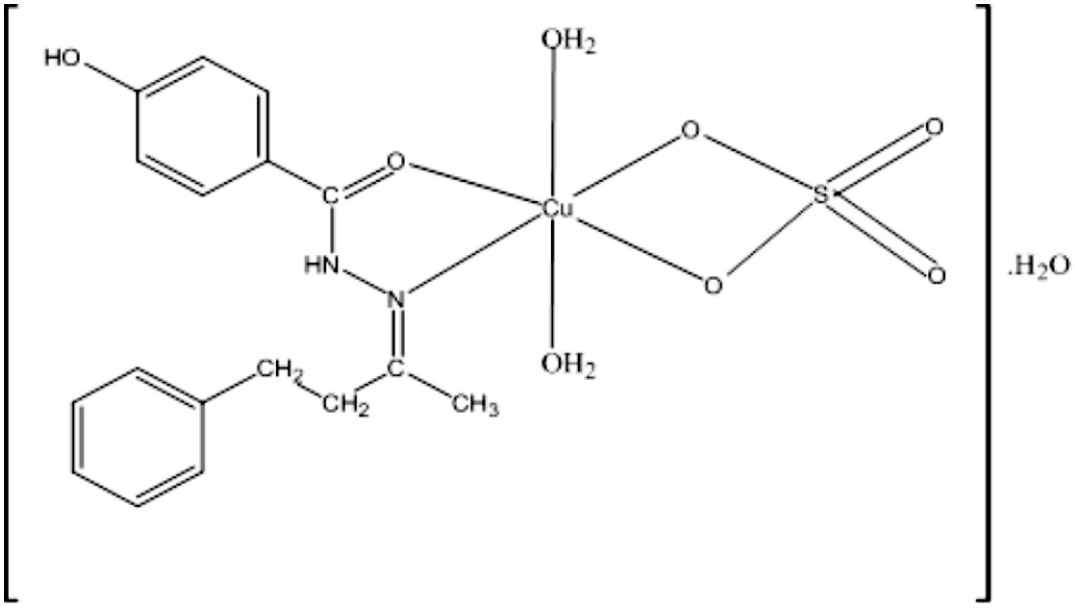

Figure 4: (a) $Cu(L^1)_2(OAc)_2$ (b) Dimeric $Cu_2(L^1)_2Cl_2$; (c) $Cu(L^2)_2Cl_2$ (d) $Cu(L^2)SO_4.3H_2O$.

REFERENCES

Adekunle, F. A. O., Semire, B. and Odunola, O. A. (2013). Synthesis, Characterization and Quantum Chemical Studies of Some Co (II) and Cu (II) Complexes of Acetoacetic Acid Hydrazide. *Asian Journal of Chemistry*, *25*(13), 7371 - 7376.

Agarwal, R. K., Sharma, D., Singh, L. and Agarwal, H. (2006). Synthesis, biological, spectral, and thermal investigations of cobalt (II) and nickel (II) complexes of N-sonicotinamido-2', 4'-dichlorobenzalaldimine. *Bioinorganic Chemistry and Applications*, *2006*.

Ajayeoba, T. A., Akinyele, O. F., Ayeni, A. O and Olawuni, I. J. (2019). Synthesis, Characterisation and Acetylcholinesterase Inhibition Activity of Nickel(II) and Copper(II) Complexes of 3-Hydroxybenzaldehyde-4 nitrobenzoic Acid Hydrazone, *American Journal of Applied Chemistry*, 7 (2): 64 - 71.

Ajayeoba, T. A., Woods J. O , Ayeni, A. O., Ajayi, T. J., Akeem, R. A., Hosten, E. C., Akinyele, O. F (2021). Synthesis, crystallographic, computational and molecular docking studies of new acetophenone-benzoylhydrazones. *Journal of Molecular Structure,* 1237: 130275.

Akinkunmi, E. O., Adesunkanmi, A. R., and Lamikanra, A. (2014). Pattern of pathogens from surgical wound infections in a Nigerian hospital and their antimicrobial susceptibility profiles. *African health sciences*, 14(4), 802-809.

Akinyele, O. F., Fakola, E. G., Durosinmi, L. M., Ajayeoba, T. A. and Ayeni, A. O. (2019). Synthesis and Characterisation of Heteroleptic metal complexes of Isoniazid and Metformin, *Ife Journal of Science*. 21 (3): 185 – 191. (Nigeria).

Akinyele, O. F., Fakola, E. G., Durosinmi, L. M., Ajayeoba, T. A**.** and Ayeni, A. O. (2020). Synthesis, characterization and antimicrobial activities of Heteroleptic metal chelates of Isoniazid and 2,2'-Bipyridine. *Bulletin of Chemical. Society of Ethiopia*. 34 (3): 471-478.

Alhadi, A. A., Shaker, S. A., Yehye, W. A., Ali, H. M. and Abdullah, M. A. (2012). Synthesis, magnetic and spectroscopic studies of Ni (II), Cu (II), Zn (II) and Cd (II) complexes of a newly Schiff base derived from 5-bromo-2hydroxybezylidene)-3,4, 5-trihydroxybenzohydrazide. *Bulletin of the Chemical Society of Ethiopia*, *26*(1), 95-101.

Al-Ne'aimi, M. M. and Al-Khuder, M. M. (2013). Synthesis, characterization and extraction studies of some metal (II) complexes containing (hydrazoneoxime and bis-acylhydrazone) moieties. *Spectrochimica Acta Part A: Molecular and Biomolecular Spectroscopy*, 105, 365-373.

Al-Sha'alan, N. H. (2011). Al-Shaalan. N. H. 2011. Synthesis, Characterization and Biological Activities of Cu(II), Co(II), and Mn(II), Fe(II), UO_2(VI) Complexes with a New Schiff Base Hydrazone: *O*-Hydroxyacetophenone-7-chloro-4 quinolineHydrazone *Molecules* 16: 8629 - 8645.

Anacona, J. R. and Rincones, M. (2015). Tridentate hydrazone metal complexes derived from cephalexin and 2-hydrazinopyridine: synthesis, characterization and antibacterial activity. *Spectrochimica Acta Part A: Molecular and Biomolecular Spectroscopy*, *141*, 169-175.

Argibay, S., Costa-Riveiro, D., Carballo, R., and Vazquez-Lopez E. M. (2022). Coordination modes of hydrazone and acyl-hydrazone ligands containing a pyridine group with the $\{Re(CO_{)3}\}^{+}$ fragment. Polyhedron 222: 115917.

Beves, J. E., Constable, E. C., Housecroft, C. E., Neuburger, M., Schaffner, S., Zampese, J.A. (2009). Substituent effects in homoleptic iron(II) and ruthenium(II) complexes of 4′ -hydrazone derivatives of 2,2′ :6′,2″-terpyridine. *Polyhedron*. 28: 3828–3838

Cao, W., Liu Y., Zhang, T., Jia, J. (2018). Synthesis, characterisation, theoretical and antimicrobial studies of tridentate hydrazone metal complexes of Zn(II), Cd(II), Cu(II) and Co(III). *Polyhedron* 147: 62 - 68.

Cao, W., Zhang, H., Yao, Q., Ge, S., Xu, J., Liu, X. and Feng, X. (2018). Catalytic enantioselective ene-type reactions of vinylogous hydrazone: construction of α methylene-γ-butyrolactone derivatives. *Chemical Communications*, *54*(88), 12511-12514.

Chitrapriya, N., Mahalingam, V., Zeller, M. and Natarajan, K. (2008). Synthesis, characterization and crystal structures of cyclometallated Ru (II) carbonyl complexes formed by hydrazones. *Polyhedron*, 27(6), 1573-1580.

Christie, R. J., Anderson, D. J. and Grainger, D. W. (2010). Comparison of hydrazineheterobifunctional cross-linking agents for reversible conjugation of thiolcontaining chemistry. *Bioconjugate chemistry*, 21(10), 1779-1787.

Chung, Y. H., Wei, H. H., Lee, G. H., Wang, Y. (1999). Magneto-structural Correlation of Dimeric Copper(II) Carboxylates with Pyridyl-substituted Nitronyl Nitroxides. *Inorganica Chimica Acta,* 293: 30 – 36.

Eflhymiou, C. G., Kito, A. A., Raptopoular, C. P., Perlepes, S. P., Escuer, A and Papatriantafyllopoulos, C. 2009. Employment of the sulphate ligand in 3d metal cluster chemistry: A novel hexanuclear nickel(II) complex with a chair metal topology. *Polyhedron* 28: 3177 - 3184.

El-Gammal, O. A., El-Reash, G. M. A., Yousef, T. A., Mefreh, M. (2015). Synthesis, spectral characterization, computational calculations and biological activity of complexes designed from NNO donor Schiff-base ligand. *Spectrochimica Acta Part A: Molecular and Biomolecular Spectroscopy*, *146:* 163-176.

El-Sherif, A. A. 2009. Synthesis, spectroscopic characterisation and biological activity on newly synthesised copper(II) and nickel(II) complexes incorporating bidentate oxygen nitrogen hydrazine Ligands. *Inorganica Chimica Acta* 362.14: 4991 –5000.

Emami, M., Shahroosvand, H., Bikas, R., Lis, T., Daneluik, C and Pilkington, M. (2021). Synthesis, Study, and Application of Pd(II) hydrazone complexes as the emissive components of single Layerlight-Emitting electrochemical cells. *Inorganic Chemistry*. 60(2): 982 – 994.

European Committee for Antimicrobial Susceptibility Testing (EUCAST) 2000. Determination of minimum inhibitory concentrations (MIC's) of antibacterial agents by agar dilution. *Clinical Microbiology and Infection* 6.9: 509 - 515.

Gup, R. and Kırkan, B. (2005). Synthesis and spectroscopic studies of copper (II) and nickel (II) complexes containing hydrazonic ligands and heterocyclic coligand. *Spectrochimica Acta Part A: Molecular and Biomolecular Spectroscopy*, 62(4-5), 1188-1195.

Gup, R., Gokce, C. and Akturk, S. (2015). Copper (II) complexes with 4-hydroxyacetophenone-derived acylhydrazones: Synthesis, characterization DNA binding and cleavage properties. *Spectrochimica Acta Part A: Molecular and Biomolecular Spectroscopy*, 134, 484-492.

Hubschle, C. B., Sheldrick, G. M. and Dittrich, B. (2011) ShelXle: A Qt Graphical User Interface for SHELXL. *Journal of Applied Crystallography* 44: 1281 – 1284.

Kendel, A., Miljanic, S., Kontrec, D., Soldin, Z., and Galic, N. (2020). Copper(II) complexes of aroylhydrazones: Preparation and structural characterization. *Journal of Molecular Structure*. 1207: 12778

Lakshmi, B., Avaji, P. G., Shivananda, K. N., Nagella, P., Manohar, S. H., Mahendra, K. N. 2011. Synthesis, spectral characterization and *in vitro* microbiological evaluation of novel glyoxal, biacetyl and benzil bis-hydrazone macrocyclic Schiff bases and their Co(II), Ni(II) and Cu(II) complexes. *Polyhedron* 30: 1507 – 1515.

Mador, S. D., Adeboye, O. O., Adejoro, I. A and B. B. Adeleke, B. B. (2019). Spectroscopic and computational studies of synthesized 2, 4 dinitropheny hydrazones of selected ketones and their derivatives. *Journal of Chemical Society*. 44 (6): 1199 -1211

Marcos A. P. Martins, Helio G. Bonacorso and Nilo Zanatta (2010) Crystal Structure, Aromatic Character and AM1 Calculations of 2-(*N*'-Benzylidenehydrazino)-4 trifluoromethyl-pyrimidine and 2-(*N*'-2 Methylbenzylidenehydrazino)-5 methyl-4 trifluoromethyl-pyrimidine. *The Open Crystallography Journal,* 2010, 3, 59-66

Mazur, L., Jarzembska, K. N., Kamiński, R., Wozniak, K., Pindelska, E and ZielińskaPisklak, M. (2014). Substituent and Solvent Effects on Intermolecular Interactions in Crystals of N-Acylhydrazone Derivatives: Single-Crystal X-ray, Solid-State NMR, and Computational Studies *Cryst. Growth Des.* 14: 2263−2281.

Meira, C. S., dos Santos Filho, J. M., Sousa, C. C., Anjos, P. S., Cerqueira, J. V., Neto, H. A. D., da Siveira, R. G., Russo, H. M., Wolfender, J-L., Queiroz, E. F., Moreira, D. R. M. and Soares, M. B. (2018). Structural design, synthesis and substituent effect of hydrazone-N-acylhydrazones reveal potent immunomodulatory agents. *Bioorganic & medicinal chemistry*, 26(8): 1971 - 1 1985

Mostafa, M. (2011). Metal Chelates of Hydrazone Ligand Chelating Tendencies of 2-Carboxyphenylhydrazoacetoacetanilide (2-Cphaaa) Ligand. *Research Journal of Chemical Sciences ISSN*, *2231*, 606X.

Nakamoto, K 1997. *Infrared and Raman Spectra of Inorganic and Coordination Compounds*. 5th Edition, New York. John Wiley and Sons Incorporated. 140 – 167.

Olurotimi, O. K., Adekoya, J. A., Agbeke, B. O., Olajumoke, O., Oluwasegun, S. T. and Sunday, E. G. (2017). Structural and Biological Activity Study of (E) N ' - (5Chloro-2 Hydroxybenzylidene) Nicotinohydrazide)[H_2L] and Some of its Divalent Metal Complexes. *Oriental Journal of Chemistry*, *33*(4), 1623.

Omoregie, O. and Woods, J. (2011). Synthesis and Physicochemical Studies of Some 2 substituted-1-phenyl-1, 3-butanedionato Nickel (II) and Copper (II) Complexes and their 2, 2'-Bipyridine and 1, 10-Phenanthroline Adducts. *International Journal of Chemistry*, *3*(1), 207.

Patel, R. N., Patel, D. K., Shodhiya, V. P., Shukla, K. K., Singh, Y., and Kumar, A. 2013. Synthesis, crystal structure and superoxide dismutase activity of two new bis(μ-acetato/μ-nitrato) bridged copper(II) complexes with N^1 [phenyl(pyridine-2-yl) methylidene]benzohydrazone. *Inorganica Chimica Acta* 405: 209 - 217

Rodriguez-Arguelles, M. C., Cao, R., Garcia-Deibe, A. M., Pelizzi, C., Matalobos, J.S., Zani, F. (2009). Antibacterial and antifungal activity of metal(II) complexes of acylhydrazones of 3-isatin and 3-(N-methyl)isatin. *Polyhedron* 28: 2187 - 2195.

Saeed, A., Arshad, M. I, Bolte, M., Fantoni A. C., Espinoza, and Z.Y.D., Erben, and M. F. (2016). On the roles of close shell interactions in the structure of acyl-substituted hydrazones: An experimental and theoretical approach. *Spectrochimica Acta Part A: Molecular and Biomolecular Spectroscopy* 157: 138 – 145.

Seleem, H. S. 2011. Transition metal complexes of an Isatinic quinolylhydrazone. *Chemistry Central Journal* 5: 35: 1 – 8.

Shebl, M., El-ghamry, M. A., Khalil, S. M. E., Kishk, M. A. A. 2014. Mono-andbinuclear copper(II) complexes of new hydrazone ligands derived from 4, 6 diacetylresorcinol: Synthesis, spectra studies and antimicrobial activity. *Spectrochimica Acta Part A: Molecular and Biomolecular Spectroscopy* 126: 232 – 241.

Sheldrick, G. M. (2015). Crystal Structure Refinement with SHELXL. *Acta Crystallographica* C, C71, 3-8.

Sheldrick, G. M. (2015). SHELXT-Integrated Space- Group and Crystal-Structure Determination. *Acta Crystallographica* Section A, A71, 3 – 8.

Wu, Y. R., Hou, L., Lan, J., Yang,F., Huang, G., Liu, W., and Gou, Y. (2023). Mixed-ligand copper(II) hydrazone complexes: Synthesis, structure, and anti-lung cancer properties. *Journal of Molecular Structure*. 1279: 134986